

Effect of Microstructure on Torsional Fatigue Endurance of Martensitic Carbon Steels and Numerical Simulation of Fatigue Crack Initiation in High Strength Steel

Shunsuke Toyoda¹, Jun'ichi Sakai²

¹ The Japan Society for Heat Treatment, ² Kagami Memorial Res. Inst. for Mater. Sci. and Technol. of Waseda University

In view of application of high strength steel tubes for automotive structural parts, the effect of microstructure of martensitic carbon steel on torsional fatigue endurance was evaluated. A laboratory vacuum-fused steel having composition of 0.1~0.2%C-0.4%Si-1.9Mn-0.2Cr-0.2Mo-0.01%P-0.001%S was hot-rolled, heated to 1023 or 1223K in a salt bath, then water quenched and tempered at 473K. Three different groups of microstructures are prepared in the type of M (martensite), M+F (ferrite), and F+P (pearlite). Fully reversed torsional fatigue test was conducted with round bar specimen of 6mm in diameter. Torsional fatigue endurance monotonously increases with the increase of tensile strength of specimen from 540 to 1380MPa. Specimens were mainly fractured precisely circumferential direction that is the maximum shear stress direction. Martensite single structure and the M+F dual-phase structure showed almost the same fatigue endurance at a tensile strength of about 950MPa. However, the morphology of fatigue micro-crack showed a little difference between them. At the surface of M+F specimen many of small cracks were observed in addition to main crack. Conversely, in martensite specimen such derivative small cracks were rarely observed. ΔK decreasing/increasing crack growth test with compact tension (CT) type specimen was also conducted. Based on these experimental results, the effects of microstructure and stress level on the initiation/propagation cycle ratio was discussed.

The fatigue endurance of TS 590 MPa grade low-alloy precipitation strengthened steel was numerically and experimentally examined. The microstructure was modeled using two-dimensional Voronoi polygons. Heterogeneous stress distributions were calculated using the finite element method, taking elastic anisotropy into consideration. The number of cycles before crack initiation was estimated based on the Tanaka–Mura model. Considering the effects of the cyclic strain of the preceding cracks, a definable macroscopic crack initiation cycle was obtained.

Keywords: high-tensile steel, torsional fatigue endurance, martensite, numerical simulation, fatigue crack initiation

1. Introduction

In order to reduce the weight and size of suspension parts, steel tubes have increasingly been used in recent years as they have a closed-section. When particularly high static strength and fatigue endurance are required, quenching is an effective method for strengthening. The effects of microstructure on fatigue endurance of steel have been investigated intensively. Kurita *et al.* investigated the effect of strengthening mechanism on fatigue endurance of F+P and F+M based microstructure with axial tension-compression mode¹. Wang *et al.* investigated the effect of martensite volume fraction and morphology on fatigue crack growth rate on F+M microstructure with tension-zero cycling².

In this study^{3),4)}, to evaluate the effect of microstructure on fatigue endurance of over 800MPa tensile strength grade steel a series of fatigue test in torsional mode and CT-type crack growth test on martensitic high-strength steels were conducted. Furthermore, the crack initiation of TS 590MPa grade low-alloy steel was numerically simulated based on Tanaka and Mura's equation.

2. Experimental procedure

The chemical composition of steels used are listed in Table 1. Small amount of micro-alloys were arbitrarily added for hardenability and grain size adjustment. Figure 1 shows hot-rolling and heat-treatment conditions of the specimens. Laboratory vacuum-fused ingots were hot-rolled, heated at 1023K or 1223K in salt bath, then water-quenched and tempered at 473K. Martensite (M), martensite and ferrite (M+F), and ferrite and pearlite (F+P) microstructures were prepared after heat treatment. The ferrite volume fractions of M+F and F+P specimens were 45% and 76%, respectively. The tensile strength varied from 540 MPa to 1380 MPa as shown Table 2.

Torsional fatigue characteristics were evaluated under stress ratio of $R = -1$ and repetition rate 33Hz condition with a 6mm ϕ round type specimen.

ΔK crack growth tests were carried out with CT-type specimen. The crack growth test was performed under sinusoidal loading at frequency of 15 Hz with stress ratio $R = 0.1$. Chemical composition is the same as FP1 and M3 in Table 1. Vickers hardness and microstructural parameters are shown in Table 3. Stepwise ΔK decreasing procedure was used to obtain threshold value. Subsequently, ΔK increasing test was conducted to obtain entire crack growth curve. Initial fatigue crack length was 12 mm and the initial ΔK value was $22 \text{ MPa}\sqrt{\text{m}}$.

Table 1. Chemical composition of steel used

Material	Chemical composition (mass %)						Microstructure [aim]
	C	Si	Mn	P	S	Others	
FP1	0.18	0.2	1.3	0.01	0.001	Cr, Ti, Nb, B	F+P
MF	0.13	1.5	1.9	0.01	0.001	Cr, Mo, Ti, Nb	M+F
M1	0.10	0.4	1.9	0.01	0.001	Cr, Mo, Ti, Nb	M
M2	0.14	0.4	1.9	0.01	0.001	Cr, Mo, Ti, Nb	
M3	0.18	0.2	1.3	0.01	0.001	Cr, Ti, Nb, B	

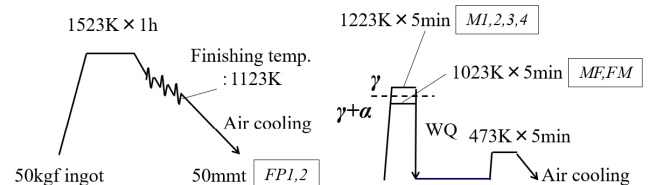


Figure 1. Hot-rolling and heat-treatment condition

Table 2. Tensile properties and microstructure of specimens

Material	Tensile properties*				HV (10)	Microstructure
	YS (MPa)	TS (MPa)	YR (%)	El (%)		
FP1	340	540	63	34	157	F+P ($V_f=76\%$, $d_f=30\mu\text{m}$)
MF	690	920	75	18	274	M+F ($V_f=45\%$, $d_f=20\mu\text{m}$)
M1	720	970	75	17	313	M
M2	890	1170	76	12	359	
M3	1110	1380	80	13	442	

*: JIS13B half; 5 mm ϕ ; gauge length = 25mm

Table 3. Hardness and microstructure of crack growth test specimens

Material	HV (10)	Microstructure
FP2	155	F+P ($V_f=75\%$, $d_f=22\mu\text{m}$)
FM	235	F+M ($V_f=65\%$, $d_f=19\mu\text{m}$)
M4	433	M

3. Results and Discussion

Figure 2 shows the relationship between stress amplitude and fatigue endurance in the torsional fatigue test. Fatigue endurance improves monotonously in accordance with tensile strength. M1 and MF, both having tensile strength about 950 MPa, show almost the same fatigue endurance independent of the loading stress level. According to SEM observation on the surface of tested specimen, the cracks of the TS 540 MPa ferrite and pearlite (FP1) specimen initiated in the ferrite grain and propagated to maximum shear stress direction. The cracks of the TS 920 MPa martensite and ferrite (MF) specimen also initiate in ferrite grain and then branched. The cracks of the TS 970 MPa martensite (M1) also indicate initiation in the shear stress direction and branching.

Figure 3 shows da/dN - ΔK curves of FP2, FM, and M4 specimens. The threshold stress intensity factor range, ΔK_{th} value decreased slightly from 10 to 8 $\text{MPa}\sqrt{\text{m}}$ with increase in hardness of the specimen. This may be due to the decrease of plastic formability at the crack tip.

To consider the reason that specimens FM and M1 shows almost the same fatigue endurance independent of the loading stress lever, the propagation cycle number was estimated based on Paris law as follows:

$$\frac{da}{dN} = C(\Delta K)^m \quad (1)$$

where C and m are material constants.

The crack propagation cycle number N_c was calculated from integration of Paris law with initial and final fatigue crack lengths as a function of nominal stress $\Delta \sigma$ for FP1, MF and M1, and M3. The calculation parameters are listed in Table 4. C and m values are extracted from the data in Figure 3 in the Paris regime.

Figure 4 shows the relationship between $\Delta \sigma$ and the calculated propagation/total cycle ratio and initiation cycle number in a log-scale. With increase in $\Delta \sigma$, the ratio of propagation cycle number increases as experimentally reported in a previous study⁵⁾. It also appears that with increase of material strength, the ratio of propagation cycle number decreases as previously reported⁶⁾.

The simple calculation readily describes the tendency of initiation/propagation fatigue phenomena. However, it is based on many assumptions and approximations. Therefore, for further quantitative estimation and discussion, many other influencing factors must be clarified and taken into account.

4. Numerical Simulation of Fatigue Crack Initiation

Prediction of fatigue-life based on microscopic mechanical and metallurgical phenomena in steel remains a

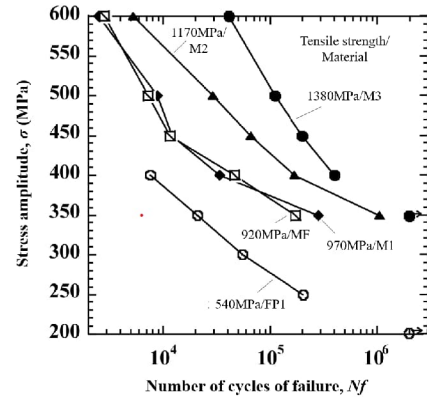


Figure 2. Relationship between stress amplitude and fatigue endurance in torsional fatigue test

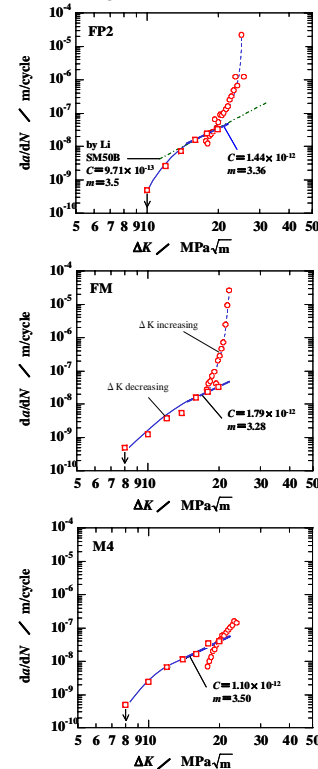


Figure 3. da/dN - ΔK curves of FP2, FM, and M4 specimens

Table 4. N_c calculation parameters

Material	Crack growth parameter			Initial and final crack length		Stress intensity factor, F
	C (m/cycle)	m	Ref.	a_i (μm)	a_c (mm)	
FP1	9.27×10^{-15}	5.05	FP2	30	3	3.34
MF-M1	9.30×10^{-14}	4.27	FM	20		
M3	1.10×10^{-12}	3.50	M4	10		

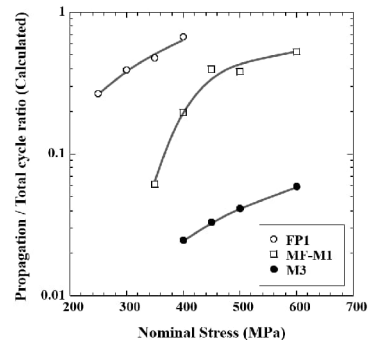


Figure 4. Relationship between $\Delta \sigma$ and the calculated propagation/total cycle ratio.

challenging research subject. One of the difficulties is in that the whole fatigue process consist of three consecutive stages: i.e. fatigue hardening and/or softening, micro-crack nucleation, and crack propagation ending in final fracture.

Tanaka and Mura⁷⁾ proposed an initiation predicting model that assumes the microcracks are initiated by irreversible dislocation pile-ups in slip bands as expressed by following equation:

$$Ni = \frac{8GW_s}{\pi(1-\nu)d(\Delta\tau - 2k)^2} \quad (2)$$

where Ni denotes the number of cycles initiation in the specific slip band, G is shear modulus, W_s is the fracture energy per unit area, ν in Poisson's ratio, d is the length of the slip band, $\Delta\tau$ is the resolved shear stress range on the slip plane, and k is the friction force of a dislocation on the slip plane. Ni corresponds to fatigue hardening and/or softening during the micro-crack nucleation stages.

In this study, the crack initiation of TS 590 MPa grade low-alloy steel was numerically simulated. By taking into account the effects of the cyclic strain of the preceding cracks, the definable macroscopic crack initiation cycle is obtained⁴⁾.

Crack initiation was numerically simulated by elasto-plastic analysis using finite element method code ABAQUS based on Eq.(2). This equation gives a Ni for each grain. Two dimensional analytical square area of $500 \times 500 \mu\text{m}$ that included about one hundred grains was modelled using the Voronoi tessellation method. The cracking slip plane was assumed to be $\{011\}$. The slip direction was inclined by 45° with respect to the principal axis of each grain's coordinate system. The potential crack path was defined as the slip plane passing through the gravity center of each grain. Von Mises yield criterion was used. The material parameters were presumed as $W_s = 2.0\text{kJ/m}^2$ and $k = 108 \text{ MPa}$.

Figure 5 shows the Mises stress distribution when one crack is generated. The figure in the parenthesis shows the latent cracking potential. The latent cracks are distributed randomly. Figure 6 shows Mises stress distribution when eight cracks are generated. Cracks tend to be clustered due to the local stress concentration induced by preexisting cracks. Local stress concentration can be seen on the fringe of the cracks. Figure 7 shows the relationship between crack density and cycle number. When the effects of the cyclic strain of the preceding cracks were taken into account by Miner's rule, the crack density increased more rapidly. An abrupt increase of crack density took place after several cracks were initiated. This abrupt increase in crack density can be considered as an actual crack initiation.

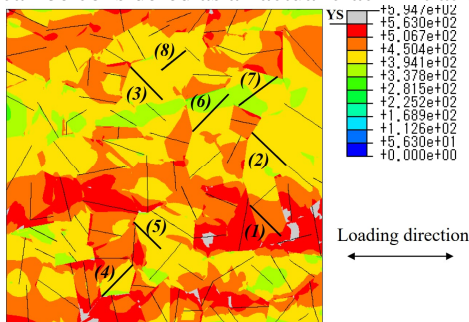


Figure 5. Mises stress distribution when one crack is generated⁴⁾

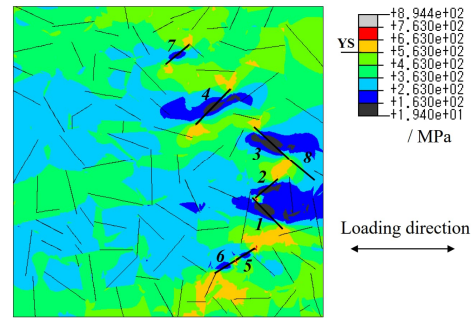


Figure 6. Mises stress distribution when eight cracks are generated⁴⁾

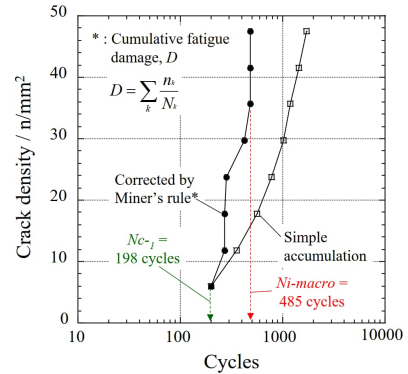


Figure 7. Relationship between crack density and cycle number⁴⁾

5. Conclusions

Torsional fatigue endurance was found to monotonously increase with increase in tensile strength in the range of 540 to 1380 MPa. Based on the crack growth test results, the propagation cycle number was calculated using the Paris law. With increase of $\Delta\sigma$ and with decrease in material strength, the ratio of propagation cycle number was found to increase based on this calculation.

Crack initiation in TS 590 MPa grade low-alloy steel was numerically simulated based on Tanaka-Mura model. By taking into account the effects of cyclic strain of the preceding cracks, definable crack initiation cycle was obtained.

Acknowledgments

The authors express the great thanks to JFE Steel Corporation where one of the authors used to belong to and previously supported this work.

References

- 1) M. Kurita, K. Toyama, S. Nomura and K. Kunishige: *Tetsu-to-Hagané*, 81-11 (1995), pp. 1091-1096
- 2) Z. G. Wang and S. H. Ai: *ISIJ Int.*, 39-8 (1999), pp. 747-759
- 3) S. Toyoda, Y. Ishiguro, Y. Kawabata, K. Sakata, A. Sato and J. Sakai: *J. Solid Mech. Mater. Eng.*, 3 (2009), pp.114-125
- 4) S. Toyoda, H. Kimura, Y. Kawabata, S. Hashimoto, N. Yoshihara and J. Sakai: *ISIJ Int.*, 50-11 (2010), pp. 1695-1701
- 5) X. Chen, I. Ohkawa and M. Misumi: *J. of Soc. Mat. Sci. Japan*, 53 (2004), pp. 199-206
- 6) T. Yokomaku and M. Kinefuchi: *Proc. of Solid Mech. JSME*, Osaka, (1993), pp. 113-114
- 7) K. Tanaka and T. Mura: *J. Appl. Mech.*, 48 (1981), pp. 97-102